Limits on the quartic couplings $Z\gamma\gamma\gamma$ and $ZZ\gamma\gamma$ from e^+e^- colliders

A. Gutiérrez-Rodríguez,[1] C. G. Honorato,[2] J. Montaño,[2] and M. A. Pérez[2]

[1] *Facultad de Física, Universidad Autónoma de Zacatecas*

Apartado Postal C-580, 98060 Zacatecas, México.

[2] *Departamento de Física, CINVESTAV.*

Apartado Postal 14-740, 07000, México D.F., México.

(Dated: April 30, 2013)

Abstract

We obtain limits on the quartic neutral gauge bosons couplings $Z\gamma\gamma\gamma$ and $ZZ\gamma\gamma$ using LEP 2 data published by the L3 Collaboration on the reactions $e^+e^- \to \gamma\gamma\gamma, Z\gamma\gamma$. We also obtain 95 % C. L. limits on these couplings at the future linear colliders energies. The LEP 2 data induce limits of order 10^{-5} for the $Z\gamma\gamma\gamma$ couplings and of order 10^{-2} for the $ZZ\gamma\gamma$ couplings, which are still above the respective Standard Model predictions. Future e^+e^- linear colliders may improve these limits by one or two orders of magnitude.

PACS numbers: 13.66.Fg, 12.15.Mm, 12.60.-i

Keywords: gauge and Higgs boson production in e^+e^- interactions, neutral currents, models beyond the standard model.

E-mail: [1]alexgu@fisica.uaz.edu.mx, [2]mperez@fis.cinvestav.mx

I. INTRODUCTION

Neutral gauge bosons self couplings provide a window to study physics beyond the Standard Model (SM) [1–3]. While trilinear neutral gauge boson couplings (TNGC) $V_iV_jV_k$, with $V_i = Z, \gamma$, test the gauge structure of the SM [3], it has been argued that quartic neutral gauge boson couplings (QNGC) $V_iV_jV_kV_l$ may provide a connection to the mechanism of electroweak symmetry breaking [1]. Since the longitudinal components of the Z gauge boson are Goldstone bosons associated to the electroweak symmetry breaking mechanism, these QNGC could represent then a connection with the scalar sector of the gauge theory that has become popular after the recent evidence of a new boson with a mass around 125 GeV [4]. However, it has been found recently in a detailed calculation of the one-loop induced decay mode $Z \to \gamma\gamma\gamma$, in both the SM and the 331 model, that the respective scalar contributions are suppressed with respect to the dominant virtual fermionic contributions [5]. This is also the case in the one-loop contributions to TNGC [3, 6]. The QNGC are induced by effective operators of dimension greater or equal to six and, in the SM, the QNGC are highly suppresed, with the only exception of the $ZZZZ$ vertex, because they arise at the one-loop level [6, 7]. Any deviation from the SM predictions for the QNGC will be associated to a signal of new physics effects [1].

While considerable effort has been devoted to study the TNGC, the QNGC are only starting to receive some attention. TNGC have been measured with an accuracy of the few percent level at LEP 2 [8] and the Tevatron [9], while QNGC are only loosely constrained at LEP 2 [8]. In fact, the $Z\gamma\gamma\gamma$ couplings have not been bounded yet by direct measurements [8]. In the present paper, we are interested in obtaining limits on the quartic vertices $Z\gamma\gamma\gamma$ and $ZZ\gamma\gamma$ coming from the LEP 2 data on the reactions $e^+e^- \to \gamma\gamma\gamma, Z\gamma\gamma$ that were used to get limits on the anomalous $HZ\gamma$ coupling but not on the QNGC [10, 11]. We will obtain also 95% C. L. limits on these quartic couplings at the future International Linear Collider (ILC) and the Compact Linear Collider (CLIC) [12, 13]. Since there is not a published account, as far as we know, of the calculation of the $Z\gamma\gamma\gamma$ vertices in the SM, in the Appendix we present a brief analysis on the connection of the $Z\gamma\gamma\gamma$ form factors to the analytical results obtained in Ref. [5] for the branching ratio of the decay mode $Z\gamma\gamma\gamma$ in both the SM and the 331 model. However, a similar calculation for the $ZZ\gamma\gamma$ form factors in the SM is not available in the published literature.

Constraints on the anomalous quartic gauge couplings $ZZ\gamma\gamma$ have been studied in $\gamma\gamma$ and $Z\gamma$ fusion processes at the LHC [14], in $ZZ\gamma$, $Z\gamma\gamma$ production processes at future e^+e^- linear colliders [6] and from the non observation of the rare decay $Z \to \nu\bar{\nu}\gamma\gamma$ at LEP 1 [7]. However, constraints on the anomalous $Z\gamma\gamma\gamma$ vertex are more difficult to get. In the present paper we find that the negative search for the reactions $e^+e^- \to \gamma\gamma\gamma, Z\gamma\gamma$ at LEP 2 by the L3 Collaboration may be translated into limits of order 10^{-5} on the $Z\gamma\gamma\gamma$ couplings and of order 10^{-2} on the $ZZ\gamma\gamma$ couplings. We also find that sensitivity studies on these couplings at future e^+e^- colliders may improve these limits by one or two orders of magnitude.

The paper is organized as follows. In Section II we present the calculation of the respective cross sections for the processes $e^+e^- \to \gamma\gamma\gamma, Z\gamma\gamma$ and in Section III we include our results and conclusions. In the Appendix we give details on the connection among our quartic couplings $G_{1,2}$ and the results obtained in Ref. [5] for the branching ratio of the decay mode $Z \to \gamma\gamma\gamma$ in the SM and the 331 model.

II. CROSS SECTIONS

We will use the following parameterizations for the QNGC [2, 15],

$$\mathcal{L}_{Z\gamma\gamma\gamma} = \frac{G_1}{\Lambda^4} F_{\mu\nu}F^{\mu\nu}F_{\rho\sigma}Z^{\rho\sigma} + \frac{G_2}{\Lambda^4} F_{\mu\nu}F^{\mu\rho}F_{\rho\sigma}Z^{\sigma\nu}, \tag{1}$$

$$\mathcal{L}_{ZZ\gamma\gamma} = -\frac{e^2}{16\Lambda^2 c_W^2} a_0 F_{\mu\nu}F^{\mu\nu}Z^{\alpha}Z_{\alpha} - \frac{e^2}{16\Lambda^2 c_W^2} a_c F_{\mu\nu}F^{\mu\alpha}Z^{\nu}Z_{\alpha}, \tag{2}$$

where $F_{\mu\nu} = \partial_\mu A_\nu - \partial_\nu A_\mu$ and $Z_{\mu\nu} = \partial_\mu Z_\nu - \partial_\nu Z_\mu$ are the respective gauge tensor fields for the photon and the Z boson. Λ represents the energy scale at which new physics interactions may appear. The respective Feynman rules for these effective vertices are thus given by,

$$\sum_{a=1}^{6} iP_a \left\{ \frac{G_1}{\Lambda^4} \Big[(p_1\cdot p_2)(p_2\cdot p_3) g_{\alpha\rho}g_{\mu\nu} - (p_1\cdot p_3) p_{1\nu}p_{2\mu}g_{\alpha\rho} - (p_1\cdot p_3) p_{1\nu}p_{2\alpha}g_{\rho\mu} + p_{1\nu}p_{1\rho}p_{2\mu}p_{3\alpha} \Big] \right.$$
$$+ \frac{G_2}{\Lambda^4} \Big[-(p_1\cdot p_2)(p_1\cdot p_3) g_{\alpha\mu}g_{\rho\nu} + (p_2\cdot p_3) p_{1\alpha}p_{1\nu}g_{\rho\mu} - (p_2\cdot p_3) p_{1\nu}p_{1\rho}g_{\alpha\mu} + (p_2\cdot p_3) p_{1\nu}p_{2\alpha}g_{\rho\mu}$$
$$\left. +2(p_2\cdot p_3) p_{1\rho}p_{2\mu}g_{\alpha\nu} - (p_1\cdot p_3) p_{1\alpha}p_{2\rho}g_{\mu\nu} - p_{1\alpha}p_{1\nu}p_{2\rho}p_{3\mu} \Big] \right\}, \tag{3}$$

and

$$\frac{ie^2}{8c_W^2\Lambda^2} \left\{ 4a_0 g^{\alpha\beta} \Big[(p_1\cdot p_2) g^{\mu\nu} - p_1^\nu p_2^\mu \Big] + a_c \Big[(p_1^\alpha p_2^\beta + p_1^\beta p_2^\alpha) g^{\mu\nu} + (p_1\cdot p_2)(g^{\mu\alpha}g^{\nu\beta} + g^{\nu\alpha}g^{\mu\beta}) \right.$$

$$- \; p_1^\nu (p_2^\beta g^{\mu\alpha} + p_2^\alpha g^{\mu\beta}) - p_2^\mu (p_1^\beta g^{\nu\alpha} + p_1^\alpha g^{\nu\beta}) \Big] \Big\} . \qquad (4)$$

All the couplings $G_{1,2}$ and $a_{0,c}$ are CP conserving and within the SM all of them vanish at tree level. As far as we know, the $a_{0,c}$ have not been computed explicitly in the SM, whereas the couplings $G_{1,2}$ can be extracted directly from the recent calculation performed in the SM and the 331 model [16] for the branching ratio of the rare decay mode $Z \to \gamma\gamma\gamma$ [5]. Since these authors did not use explicitly the parametrization given in Eqs. (1) and (2), we have included in the Appendix the connection of the $G_{1,2}$ couplings to the results obtained for the $Z \to \gamma\gamma\gamma$ decay in Ref. [5]. These form factors are dominated by the fermionic virtual contributions and they are essentially the same in both the SM and the 331 model, but unfortunately with rather low values, 1.63×10^{-10} and 1.33×10^{-10}, respectively.

In Figures 1 and 2 we present the contributions of the effective interactions given in Eqs. (3) and (4) to the processes $e^+e^- \to \gamma\gamma\gamma$ and $e^+e^- \to Z\gamma\gamma$. The SM contributions to these processes occur via t-channel diagrams involving initial-state radiation [2, 6]. The respective SM cross sections have been computed by Stirling and Werthenbach for CM energies greater than 200 GeV [6]. They are of order of few femtobarns. According to this result, in order to reduce the contributions due to initial-state radiation in these reactions, the L3 Collaboration introduced cuts on the photon energies and their polar angles, $E_\gamma > 5$ GeV and $|\cos\theta_\gamma| < 0.97$ [10]. Events from $e^+e^- \to \gamma\gamma\gamma, Z\gamma\gamma$ processes were selected by requiring the photon candidates to lay in the central region of the detector with $|\cos\theta_\gamma| < 0.8$ and a total CM electromagnetic energy large than $\sqrt{s}/2$. In this case, the L3 Collaboration was interested in getting limits on the anomalous Higgs couplings $HZ\gamma$ and $H\gamma\gamma$. However, using their data we are able to get also limits on the $G_{1,2}$ and $a_{0,c}$ couplings: $G_1/\Lambda^4 < 1.2 \times 10^{-5}$, $G_2/\Lambda^4 < 9.4 \times 10^{-6}$, $a_0/\Lambda^2 < 5.9 \times 10^{-3}$ and $a_c/\Lambda^2 < 1.6 \times 10^{-2}$. The latter limits should be compared with the more stringent bounds obtained by the L3 Collaboration from a direct search of $Z\gamma\gamma$ events at LEP 2 energies: [-0.08, 0.021] and [-0.029, 0.039], respectively [8].

The expressions for the respective cross sections induced by the effective vertices given in Eqs. (3) and (4) are given by

$$\sigma(e^+e^- \to \gamma\gamma\gamma) = \frac{\alpha M_Z^{10}}{1105920\pi^2} \left[\frac{1 - 4x_W + 8x_W^2}{x_W(1 - x_W)} \right] \left[\frac{2\left(\frac{G_1}{\Lambda^4}\right)^2 + 3\left(\frac{G_2}{\Lambda^4}\right)^2 - 3\left(\frac{G_1}{\Lambda^4}\right)\left(\frac{G_2}{\Lambda^4}\right)}{(s - M_Z^2)^2 + M_Z^2\Gamma_Z^2} \right], \quad (5)$$

and

$$\sigma(e^+e^- \to Z\gamma\gamma) = \frac{\alpha M_Z^6 (s-M_Z^2)^4}{5308416\pi^2 s^4}\left[71\left(\frac{G_1}{\Lambda^4}\right)^2 + 138\left(\frac{G_1}{\Lambda^4}\right)\left(\frac{G_2}{\Lambda^4}\right) + 96\left(\frac{G_2}{\Lambda^4}\right)^2\right]$$
$$+ \frac{5\alpha M_Z^6 (s-M_Z^2)^4}{4608\pi^2 s^4\left[(s-M_Z^2)^2 + M_Z^2\Gamma_Z^2\right]}\left[\frac{1-4x_W+8x_W^2}{x_W(1-x_W)}\right]$$
$$\times \left[\frac{a_0^2}{\Lambda^4} + \frac{1}{8}\frac{a_c^2}{\Lambda^4} + \frac{1}{2}\frac{a_c}{\Lambda^2}\frac{a_0}{\Lambda^2}\right]. \quad (6)$$

In Eq. (6), the first term comes from the Feynman diagrams shown in Fig. 2 for the exchanged photon and the second one comes from the exchanged Z boson. We did not include the contribution coming from the interference of the two diagrams because we will get limits on the form factors one at the time.

III. RESULTS AND CONCLUSIONS

Using the numerical values $\sin^2\theta_W = x_W = 0.2314$, $M_Z = 91.18\ GeV$ and $\Gamma_Z = 2.49\ GeV$ [17], we obtain the cross sections for the processes $e^+e^- \to \gamma\gamma\gamma, Z\gamma\gamma$ as functions of the CM energy and the $G_{1,2}, a_{0,c}$ couplings. We have also implemented in our calculation the cut used by the L3 Collaboration on the CM energy and the photon polar angle in order to suppress the SM contributions associated to initial-state radiation. In Fig. 3 we depict the sensitivity limits at 95 % $C.L.$ for the $G_{1,2}$ couplings for CM energies of 500 GeV and 1000 GeV and we have taken the $G_{1,2}$ couplings one at the time. The respective combined limits contours are shown in Fig. 4. On the other hand, in order to get sensitivity limits and the respective limits contours for the $a_{0,c}$ couplings we have set to zero the contribution associated to the $G_{1,2}$ couplings in Eq. (6). The respective limits are given in Figures 5 and 6 also for two different values of the energy of the ILC and CLIC acelerators.

In conclusion, we have obtained limits on the quartic couplings $Z\gamma\gamma\gamma$ and $ZZ\gamma\gamma$ at LEP 2 energies by using published L3 data for the reactions $e^+e^- \to \gamma\gamma\gamma, Z\gamma\gamma$. However, our limits for the $Z\gamma\gamma\gamma$ couplings are five orders of magnitude above the expected predictions for the SM included in our Appendix. In the case of the $ZZ\gamma\gamma$ couplings, our limits obtained from the LEP 2 data on the reaction $e^+e^- \to Z\gamma\gamma$ are still one order of magnitude above the best limits obtained in LEP collider [8]. On the other hand, these limits may be improved by one or two orders of magnitude at future linear colliders (Figure 6). Similar limits have been obtained for the $a_{o,c}$ couplings from the process $e^+e^- \to \nu\bar{\nu}\gamma\gamma$ [18] and through effects

induced by the polarization of the Z gauge boson and initial state radiation in the process $e^+e^- \to Z\gamma\gamma$ [19].

Acknowledgments

We acknowledge support from CONACyT, SNI and PROMEP (México).

Appendix A: $Z \to \gamma\gamma\gamma$ at one-loop level

The branching ratio for the decay $Z \to \gamma\gamma\gamma$ was obtained in Ref. [5] for the SM and the 331 model to one-loop order. In this appendix we present some details of the calculation that leads to the values obtained for the quartic coupling constant G_i/Λ^4, $i = 1, 2$, defined in Eq. (1). In Ref. [5] this calculation was performed in terms of the form factors F_{Z_i} which identify the fermionic, vectorial, and scalar components of the respective Feynman amplitudes,

$$F_{Z_i} = F_{Z_i}^{1/2} + F_{Z_i}^{1} + F_{Z_i}^{0} \ , \tag{A1}$$

with

$$F_{Z_i}^{1/2} = \sum_{F=q,Q,l} g_{1/2}^{F} f_{Z_i}^{F} = F_{Z_i}^{q} + F_{Z_i}^{Q} + F_{Z_i}^{l} \ . \tag{A2}$$

The fermionic contribution $F_{Z_i}^{1/2}$ is expresed in terms of the light quarks $q = u, d, s, c, b, t$, the new heavy quarks of the 331 model $Q = D, S, T$, and the leptones $l = e, \mu, \tau$, with

$$g_{1/2}^{F} \equiv -N_F Q_F^3 g_Z^F \ , \tag{A3}$$

where Q_{F_i} is the respective fermionic charge and g_Z^F correspond to the fermionic coupling constants to the neutral gauge boson Z and Z'. The vectorial form factor $F_{Z_i}^{1}$ is splited in the contributions of the charged W boson and the respective degenerated bileptons Y^+ and Y^{++}, and their correspondent pseudoscalars

$$\begin{aligned} F_{Zi}^{1} &= F_{Zi}^{W} + F_{Zi}^{Y} \\ &= [2c_W^2 f_{Zi}^{W} - c_{2W} f_{Zi}^{G_W}] + [(7 - 34 s_W^2)(f_{Zi}^{Y} - f_{Zi}^{G_Y})] \ . \end{aligned} \tag{A4}$$

Finally, the scalar form factor $F_{Z_i}^{0}$ is given in terms of the charged Higgs bosons $H = h_1^+$, h_2^+, h_3^+, h_4^+, d_1^{++}, d_2^{++}, d_3^{++},

$$\begin{aligned} F_{Zi}^{0} &= F_{Zi}^{H} \\ &= 2(9 - 52 s_W^2) f_{Zi}^{h} \ . \end{aligned} \tag{A5}$$

The form factors $f_{Z_i}^F$ are given in Ref. [19], and $f_{Z_i}^{W,Y,G^W,G^Y,h}$ in the appendix of Ref. [5].

The relation between the effective form factors G_i/Λ^4 and the F_{Z_i} form factors calculated in Ref. [5] is given by the integral expression

$$\left(\frac{G_{1,2}}{\Lambda^4}\right)^2 = 2\Big[\frac{8\alpha^2(M_Z)}{s_W c_W}\Big]^2 \int_0^1 \int_{1-x}^1 \Big|F^{\frac{1}{2}}_{ZG_{1,2}} + F^1_{ZG_{1,2}} + F^0_{ZG_{1,2}}\Big|^2 dydx \ , \tag{A6}$$

where the x and y are the kinematical variables asociated to the $Z \to \gamma\gamma\gamma$ decay amplitude [5], and $g = e/s_W = \sqrt{4\pi\alpha}/s_W$.

In the Tables I-VII we show the results obtained for each one of the contributions of the G_i/Λ^4 form factors for the SM and the 331 model.

The branching ratio predicted for the $Z \to \gamma\gamma\gamma$ decay in these models is obtained with the relation

$$\mathrm{Br}(Z \to \gamma\gamma\gamma) = \frac{\Gamma(Z \to \gamma\gamma\gamma)}{\Gamma_0} \ , \tag{A7}$$

and the decay width [15, 20]

$$\Gamma(Z \to \gamma\gamma\gamma) = \frac{M_Z^9}{552960\pi^3}\frac{(2G_1^2 + 3G_2^2 - 3G_1G_2)}{\Lambda^8} \ , \tag{A8}$$

and the experimental total Z width [17] is

$$\Gamma_0 = 2.4952\, GeV. \tag{A9}$$

In Table VIII we give the predictions obtained for the G_i/Λ^4 $[GeV^{-4}]$ form factor from the branching ratio (A7).

TABLE I: Predictions of the 331 model to the $G_{1,2}/\Lambda^4$ $[GeV^{-4}]$ couplings and the respective BR($Z \to \gamma\gamma\gamma$) from the fermionic, bosonic and scalar sectors. BR with Eq. (A8).

Sector	$\lvert G_1/\Lambda^4\rvert$	$\lvert G_2/\Lambda^4\rvert$	BR
Fermions	6.06×10^{-10}	8.66×10^{-10}	1.44×10^{-8}
Gauge Bosons	1.41×10^{-12}	1.75×10^{-11}	8.65×10^{-12}
Scalar	6.24×10^{-14}	1.27×10^{-13}	3.30×10^{-16}
Fermions-Gauge Bosons	2.65×10^{-11}	1.12×10^{-10}	3.07×10^{-10}
Fermions-Scalar	6.10×10^{-12}	1.15×10^{-11}	2.66×10^{-12}
Gauge Bosons-Scalar	1.82×10^{-13}	4.37×10^{-13}	4.08×10^{-15}
Total	6.06×10^{-10}	8.74×10^{-10}	1.46×10^{-8}

TABLE II: Predictions of the 331 model to the $G_{1,2}/\Lambda^4$ $[GeV^{-4}]$ couplings and the respective BR($Z \to \gamma\gamma\gamma$) from fermionic subsectors. BR with Eq. (A8).

Fermions	$\lvert G_1/\Lambda^4\rvert$	$\lvert G_2/\Lambda^4\rvert$	BR
Quarks	4.75×10^{-10}	6.73×10^{-10}	8.67×10^{-9}
Leptones	1.42×10^{-10}	2.03×10^{-10}	7.89×10^{-10}
Quarks-Leptons	3.50×10^{-10}	5.06×10^{-10}	4.91×10^{-9}
Total	6.06×10^{-10}	8.66×10^{-10}	1.44×10^{-8}

TABLE III: Predictions of the 331 model to the $G_{1,2}/\Lambda^4$ $[GeV^{-4}]$ couplings and the respective BR($Z \to \gamma\gamma\gamma$) from quarks subsectors. BR with Eq. (A8).

Quarks	$\lvert G_1/\Lambda^4\rvert$	$\lvert G_2/\Lambda^4\rvert$	BR
SM quarks	4.73×10^{-10}	6.70×10^{-10}	8.59×10^{-9}
Exotic quarks	2.35×10^{-12}	5.15×10^{-12}	5.53×10^{-13}
SM-exotic quarks	3.35×10^{-11}	6.28×10^{-11}	7.91×10^{-11}
Total	4.75×10^{-10}	6.73×10^{-10}	8.67×10^{-9}

TABLE IV: Predictions of the 331 model to the $G_{1,2}/\Lambda^4$ $[GeV^{-4}]$ couplings and the respective BR($Z \to \gamma\gamma\gamma$) from gauge bosons. BR with Eq. (A8).

Bosons	$\lvert G_1/\Lambda^4\rvert$	$\lvert G_2/\Lambda^4\rvert$	BR
W	1.42×10^{-12}	1.76×10^{-11}	8.75×10^{-12}
Bileptons	4.44×10^{-14}	1.28×10^{-13}	3.67×10^{-16}
W-Bileptons	1.66×10^{-13}	1.79×10^{-12}	8.94×10^{-14}
Total	1.41×10^{-12}	1.75×10^{-11}	8.65×10^{-12}

TABLE V: Predictions of the SM to the $G_{1,2}/\Lambda^4$ $[GeV^{-4}]$ couplings and the respective BR($Z \to \gamma\gamma\gamma$). BR with Eq. (A8).

SM	$\lvert G_1/\Lambda^4\rvert$	$\lvert G_2/\Lambda^4\rvert$	BR
Quarks	4.73×10^{-10}	6.70×10^{-10}	8.59×10^{-9}
Leptons	1.42×10^{-10}	2.03×10^{-10}	7.89×10^{-10}
W	1.42×10^{-12}	1.76×10^{-11}	8.75×10^{-12}
Quarks-Leptons	3.49×10^{-10}	5.05×10^{-10}	4.89×10^{-9}
Quarks-W	2.31×10^{-11}	1.00×10^{-10}	2.46×10^{-10}
Leptons-W	1.19×10^{-11}	5.16×10^{-11}	6.55×10^{-11}
Total	6.04×10^{-10}	8.71×10^{-10}	1.45×10^{-8}

TABLE VI: Predictions of the SM to the $G_{1,2}/\Lambda^4$ $[GeV^{-4}]$ couplings and the respective BR($Z \to \gamma\gamma\gamma$) from quarks. BR with Eq. (A8).

SM quarks	$\lvert G_1/\Lambda^4\rvert$	$\lvert G_2/\Lambda^4\rvert$	BR
u	3.11×10^{-10}	4.43×10^{-10}	3.76×10^{-9}
c	2.58×10^{-10}	3.18×10^{-10}	1.94×10^{-9}
t	1.85×10^{-14}	2.11×10^{-14}	8.65×10^{-18}
d	7.02×10^{-11}	1.00×10^{-10}	1.92×10^{-10}
s	7.50×10^{-11}	1.07×10^{-10}	2.19×10^{-10}
b	1.86×10^{-11}	2.43×10^{-11}	1.13×10^{-11}
Interference	2.23×10^{-10}	3.60×10^{-10}	2.52×10^{-9}
Total	4.73×10^{-10}	6.70×10^{-10}	8.59×10^{-9}

TABLE VII: Predictions of the SM to the $G_{1,2}/\Lambda^4$ $[GeV^{-4}]$ couplings and the respective BR($Z \to \gamma\gamma\gamma$) from leptons. BR with Eq. (A8).

Leptons	$\lvert G_1/\Lambda^4\rvert$	$\lvert G_2/\Lambda^4\rvert$	BR
e	6.88×10^{-11}	9.80×10^{-11}	1.84×10^{-10}
μ	7.39×10^{-11}	1.06×10^{-10}	2.15×10^{-10}
τ	4.05×10^{-11}	5.10×10^{-11}	4.98×10^{-11}
Interf.	9.12×10^{-11}	1.33×10^{-10}	3.39×10^{-10}
Total	1.42×10^{-10}	2.03×10^{-10}	7.89×10^{-10}

TABLE VIII: Values of $G_{1,2}/\Lambda^4$ $[GeV^{-4}]$ as function of BR according to Eq. (16) of Ref. [15]. We include the PDG 2012 limit for BR($Z \to \gamma\gamma\gamma$) [17].

BR	$\lvert G_1/\Lambda^4\rvert$	$\lvert G_2/\Lambda^4\rvert$
10^{-5}(PDG)	2.22×10^{-8}	1.81×10^{-8}
5.41×10^{-10}(SM)	1.63×10^{-10}	1.33×10^{-10}
5.26×10^{-10}(3-3-1)	1.61×10^{-10}	1.31×10^{-10}

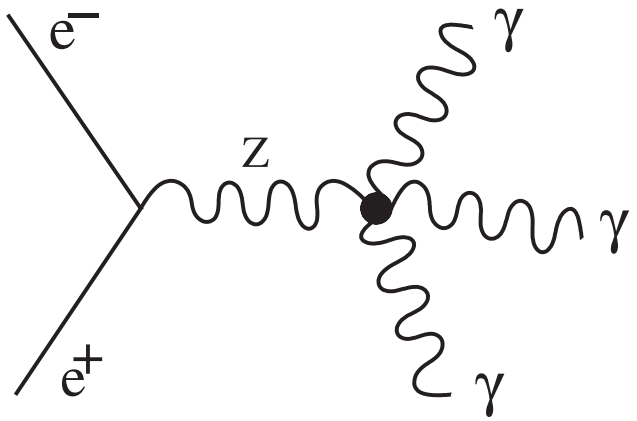

FIG. 1: Feynman diagram for the process $e^+e^- \to \gamma\gamma\gamma$ induced by the effective vertex $Z\gamma\gamma\gamma$.

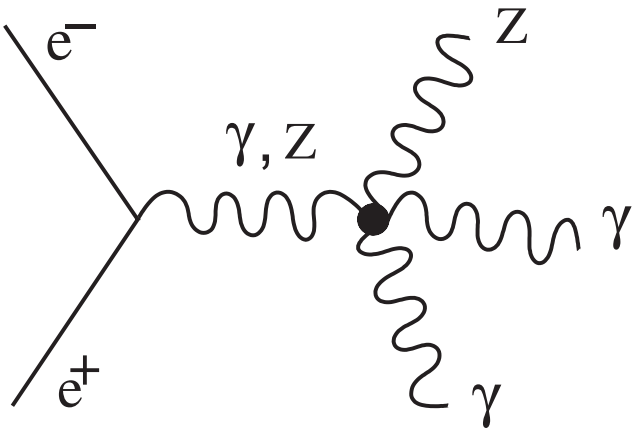

FIG. 2: Feynman diagrams for the process $e^+e^- \to Z\gamma\gamma$ induced by the effective vertices $ZZ\gamma\gamma$ and $Z\gamma\gamma\gamma$.

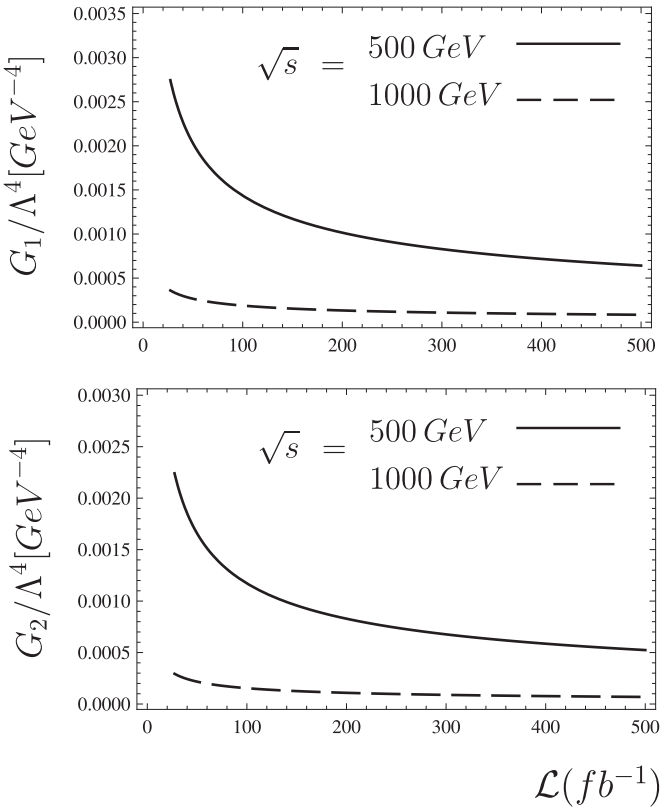

FIG. 3: Sensitivity limits at 95 % C.L. for the couplings $\frac{G_{1,2}}{\Lambda^4}[GeV^{-4}]$ as function of the integrated luminosity for two ILC/CLIC CM energies.

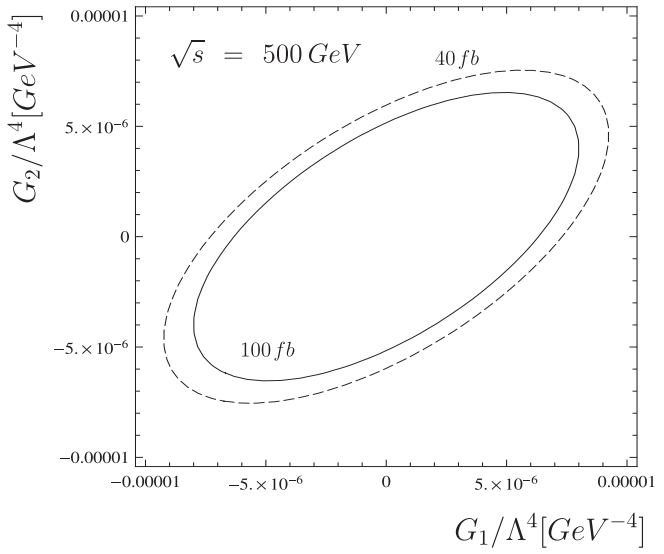

FIG. 4: Contours limits at 95 % C. L. in the G_1-G_2 plane for the process $e^+e^- \to \gamma\gamma\gamma$ for two values of the cross section, 40 and 100 fb and $\sqrt{s} = 500\,GeV$.

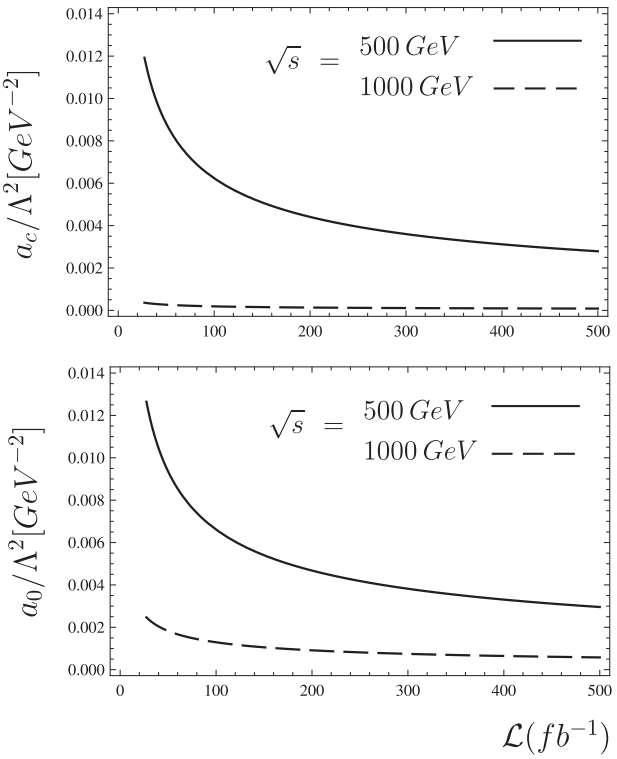

FIG. 5: Sensitivity limits at 95 % C.L. for the couplings $\frac{a_{0,c}}{\Lambda^2}[GeV^{-2}]$ as function of the integrated luminosity for two ILC/CLIC CM energies.

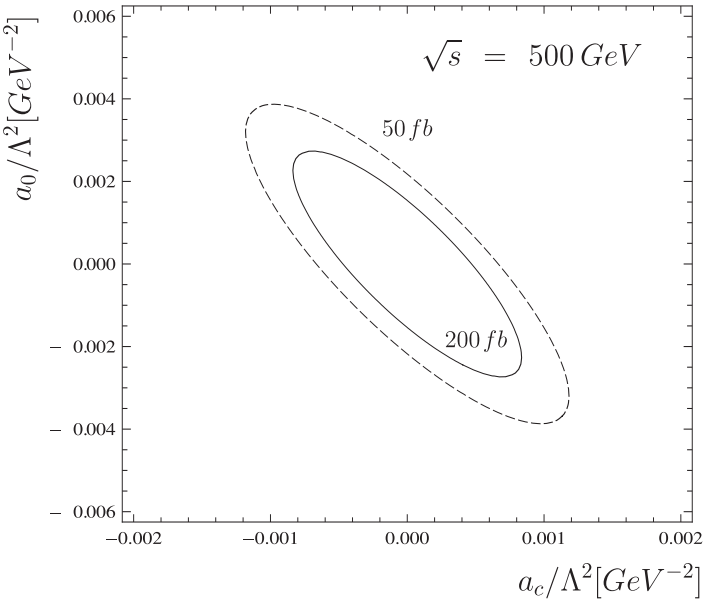

FIG. 6: Contours limits at 95 % C. L. in the a_0-a_c plane for the process $e^+e^- \to Z\gamma\gamma$ for two values of the cross section, 50 and 200 fb and $\sqrt{s} = 500\,GeV$.

[1] J. Ellison and J. Wudka, *Annu. Rev. Nucl. Part. Sci.* **4**8, 33 (1998); G. Weiglein *et al.*, LHC/ILC Study Group, *Phys. Rept.* **426**, 47 (2006); S. Godfrey, AIP Conf. Proc. 350, 41 (1995); arXiv:hep-ph/9505252; J. J. Toscano, *AIP Conf. Proc.* **857B**, 103 (2006).

[2] A. Barroso *et al.*, *Z. Phys.* **C28**, 149 (1985).

[3] J. M. Hernández, *et al.*, *Phys. Rev.* **D60**, 013004 (1999); G. J. Gounaris, *et al.*, *Phys. Rev.* **D62**, 073013 (2000); F. Larios, *et al.*, *Phys. Rev.* **D63**, 113014 (2001); M. A. Pérez, G. Tavares Velasco and J. J. Toscano, *Int. J. Mod. Phys.* **A19**, 159 (2004); O. Cata, arXiv:1304.1008 [hep-ph].

[4] G. Aad, *et al.*, ATLAS Collaboration, *Phys. Lett.* **B716**, 1 (2012); S. Chatrchyan, *et al.*, CMS Collaboration, *ibid.* **30**, (2012).

[5] J. Montaño, *et al.*, *Phys. Rev.* **D85**, 035012 (2012); A. Denner, *et al.*, *Eur. Phys. J.* **C20**, 201 (2001).

[6] G. Belanger, F. Boudjema, *Phys. Lett.* **B288**, 201 (1992); W. J. Stirling, A. Werthenbach, *Eur. Phys. J.* **C14**, 103 (2000); G. Montagna, *et al.*, *Nucl. Phys.* **B541**, 31 (1999).

[7] M. A. Pérez, G. Tavares-Velasco, and J. J. Toscano, *Phys. Rev.* **D67**, 017702 (2003).

[8] S. Villa, *Nucl. Phys.* **B** (Proc. Suppl.) **142**, 391 (2005), and references therein.

[9] V. M. Abasov, *et al.*, D0 Collaboration, *Phys. Lett.* **B653**, 378 (2007); D. Acosta, *et al.*, CDF Collaboration, *Phys. Rev. Lett.* **94**, 041803 (2005).

[10] P. Achard *et al.*, L3 Collaboration, *Phys. Lett.* **B589**, 89 (2004); *ibid*, *Phys. Lett.* **B540**, 43 (2002).

[11] A. Gutiérrez-Rodríguez, J. Montaño and M. A. Pérez, *J. Phys. G: Nucl. Part. Phys.* **G38**, 095003 (2011).

[12] T. Abe, *et al.*, American Linear Collider Group, hep-ex/0106057; J. A. Aguilar-Saavedra, *et al.*, ECFA/DESY Lc Physics Working Group, hep-ph/0106315; Koh Abe, *et al.*, ACFA Linear Collider Working Group, hep-ph/0109166; ILC Technical Review Committee, second report, 2003, SLAC-R-606, February 2003; E. Accomando, *et al.*, CLIC Physics Working Group, hep-ph/0412251.

[13] J. E. Abreu, *et al.*, arXiv:1210.0202 [hep-ex].

[14] E. Chapon, C. Royon, O. Kepka, *Phys. Rev.* **D81**, 074003 (2010); I. Sahin and B. Sahin, *Phys.*

Rev. **D86**, 115001 (2012); R. S. Gupta, *Phys. Rev.* **D85**, 014006 (2012).

[15] M. Stohr and J. Horejsí, *Phys. Rev.* **D49**, 3775 (1994); J. Horejsí, M. Stohr, *Z. Phys.* **C64**, 407 (1994).

[16] F. Pisano and V. Pleitez, *Phys. Rev.* **D46**, 410 (1992); H. Frampton, *Phys. Rev. Lett.* **69**, 2889 (1992).

[17] J. Beringer, *et al.*, Particle Data Group, *Phys. Rev.* **D86**, 010001 (2012).

[18] G. Montagna, *et al.*, *Phys. Lett.* **B515**, 197 (2001).

[19] M. Baillargeon *et al.*, *Z. Phys.* **C71**, 431 (1996).

[20] A. Flores-Tlalpa, J. Montaño, F. Ramirez-Zavaleta and J. J. Toscano, *Phys. Rev.* **D80**, 033006 (2009).